

# Modellazione numerica del flusso idrico nell'acquifero fratturato e carsico della penisola Salentina (Sud Italia)

## *Numerical modeling of the groundwater flow in the fractured and karst aquifer of the Salento peninsula (Southern Italy)*

Giovanna De Filippis, Mauro Giudici, Stefano Margiotta, Fiorella Mazzone, Sergio Negri e Chiara Vassena

**Riassunto:** Le risorse idriche rappresentate dagli acquiferi costieri sono estremamente importanti per quelle regioni caratterizzate da una forte richiesta di acqua dolce, ma da limitate precipitazioni, da carenza di corpi idrici superficiali e dall'intrusione di acqua di mare nei sedimenti che ospitano le acque di falda. Per questo alcune aree costiere, come la penisola Salentina (sud Italia), sono soggette al rischio di desertificazione e una gestione sostenibile delle risorse idriche sotterranee richiede strumenti di analisi e previsione del bilancio idrico e dell'evoluzione del sistema fisico in risposta ad attività antropiche (ad esempio, i prelievi) e a fattori climatici.

La penisola Salentina è un bacino nel cuore del Mediterraneo e la sua principale riserva idrica è l'acquifero ospitato all'interno di rocce carbonatiche che risalgono all'epoca del Cretaceo (Calcere di Altamura): si tratta di un acquifero fratturato e carsico, con scarsa ricarica e complesse relazioni con il mare.

**Parole chiave:** acquiferi costieri, bilancio idrico, modellazione numerica, modello concettuale, Salento.

**Keywords:** *coastal aquifers, water budget, numerical modeling, conceptual model, Salento.*

**Giovanna DE FILIPPIS** 

Dipartimento di Scienze della Terra, Università degli Studi di Milano  
giovanna.defilippis@unimi.it

**Mauro GIUDICI**

Dipartimento di Scienze della Terra, Università degli Studi di Milano  
Consorzio Interuniversitario Nazionale per la Fisica delle Atmosfere e delle Idrosfere, Camerino  
mauro.giudici@unimi.it

**Fiorella MAZZONE**

Geomod srl, Lecce  
fiorella.mazzone@unisalento.it

**Stefano MARGIOTTA**

**Sergio NEGRI**

Laboratorio di idrogeofisica e stratigrafia per i rischi naturali, DiSTeBa,  
Università del Salento, Lecce  
stefano.margiotta@unisalento.it  
sergio.negri@unisalento.it

**Chiara VASSENA**

Consorzio Interuniversitario Nazionale per la Fisica delle Atmosfere e delle Idrosfere, Camerino  
chiara.vassena@guest.unimi.it

Ricevuto: 29 novembre 2012 / Accettato: 20 febbraio 2013

Publicato online: 31 marzo 2013

© Associazione Acque Sotterranee 2013

Per sviluppare uno strumento di analisi del bilancio idrico su scala regionale per questo sistema acquifero, un primo modello di flusso delle acque sotterranee è stato sviluppato da Giudici et al. (2012a); tale modello è basato su un modello concettuale ottenuto da una ricostruzione dell'architettura idrostratigrafica della regione, che comprende l'acquifero principale e le rocce sovrastanti a bassa permeabilità che possono ospitare acquiferi locali e con spessori relativamente piccoli.

In questo lavoro viene presentato un ulteriore stadio di sviluppo del modello, attraverso un miglioramento nella ricostruzione dell'altezza idraulica e del modello concettuale nelle aree dove la prima versione del modello indicava situazioni critiche, ovvero dove l'acquifero appare saturo di acqua salata su tutto il proprio spessore. Inoltre, la stima di alcuni parametri di ingresso del modello può essere condizionata da una notevole incertezza e quindi viene presentata un'analisi di sensibilità per valutare gli effetti di tale incertezza sui risultati del modello stesso.

**Abstract:** *Water resources represented by coastal aquifers are very important for regions characterized by a relevant request of freshwater, but limited rainfall, lack of surface water bodies and intrusion of the seawater through the sediments which host groundwater. Therefore some coastal areas, like the Salento peninsula (southern Italy), are subjected to the risk of desertification and a proper management of groundwater resources requires tools to analyze and predict the water balance and the evolution of the physical system in response to human activities (e.g., ground water withdrawals) and climatic factors.*

*The Salento peninsula is a typical Mediterranean basin, where the main water resource is the aquifer hosted in Cretaceous carbonatic rocks (Calcere di Altamura, Altamura limestone): this is a fractured and karst aquifer, with a poor recharge and complex relationships with the sea.*

*In order to develop a tool to assess the water balance at regional scale for the considered aquifer system, a groundwater flow model was developed by Giudici et al. (2012a); it is based on a conceptual model obtained from a reconstruction of the hydrostratigraphic architecture of the region, which includes the main aquifer and the overlying rocks characterized by low permeability which can host local and relatively thin aquifers.*

*In this paper that work is updated, by improving the reconstruction of the hydraulic head and of the conceptual model, above all in those areas that the previous model evidenced as critical for the absence of fresh water along the whole aquifer thickness. Moreover, since the estimate of some model's input parameters is affected by high uncertainty, a sensitivity analysis is performed to evaluate the effects of this uncertainty on the model's results.*

## Introduction

The heavy urbanization and the presence of active industrial and touristic systems in coastal areas increase the pressure on groundwater resources (Andreo and Duràn, 2008; Bakalowicz et al., 2008; Daskalaki and Voudouris, 2008; Davraz et al., 2009; Custodio, 2010). Moreover, many coastal areas in the Mediterranean region suffer from limited precipitations, high evapotranspiration rates and poor surface water bodies and resources, so that the risk of desertification is very high. The correct evaluation of the global water cycle, including groundwater (Church et al., 1995; Younger, 1996; Post and Abarca, 2010; Custodio, 2010), is fundamental to simulate the dynamics of the interface between fresh and salt water, to estimate the fresh water discharge towards the sea, and, possibly, to develop and apply proper decision support systems for the management of water resources.

The Salento peninsula (southeastern Italy, Fig.1) is a typical Mediterranean basin, which is bounded to the east side by the Adriatic sea, to the west side by the Ionian sea and to the north side by the Murge hills. The region is characterized by a modest availability of surface water resources because of the mainly karst nature of its territory. However, considerable resources of fresh water are located in the coastal carbonate aquifers and cover more than 65% of the total water demand (Delle Rose et al., 2003). The lack of surface water bodies and the relative richness of groundwater expose subsurface water to the risk of widespread and excessive withdrawals. In fact, groundwater was extracted in significant and increasing amounts over the years for domestic, agricultural and industrial uses, allowing the civil and economic growth of the local population (Polemio et al., 2006). This, in turn, led to growing salt contamination resulting from the continental invasion of seawater through the underground karst channels, which may represent routes of rapid and deep saline intrusion

(Margiotta and Negri, 2005). The increasing use of groundwater, together with the pollution generated by human activities and the climatic changes that have led to a decrease in aquifer recharge all over southern Italy since 1980, makes the risk of deterioration of groundwater quality and quantity more realistic (Polemio et al., 2012). A careful management and the proper use of groundwater are therefore matters of great importance.

The vulnerability of Salento aquifer to seawater intrusion was studied in several papers, Polemio et al. (2012) and Cotecchia et al. (2005) among the others. Furthermore, Margiotta and Negri (2005) characterized the aquifer by monitoring the piezometric level, salinity, pH and dissolved oxygen values and the volume of fresh water by using geophysical surveys. Moreover, a first mathematical model of groundwater flow for the carbonatic aquifer of the peninsula at regional scale was developed by Giudici et al. (2012a) and then improved by De Filippis (2012), taking into account the complex hydrostratigraphic architecture and hydrogeological conditions both inland and along the coast.

It is important to recall that the ultimate goal of these works is to develop a reliable tool to support planning decisions by central and local governments about the management of the main water resource of the Salento peninsula. In other words, from the hydrogeological point of view, the general aim is to develop a large-scale model which estimates the water balance at the scale of a hydrogeological basin. Therefore, such a model is different not only from the mathematical models which are used to study coastal aquifers at the local scale, mainly to determine the impact of pumping on salt water intrusion (Vandenbohede et al., 2009; Yuan and Lin, 2009; among the others), but also from modeling studies that are found in the literature and deal with catchments whose size is up to 200 km<sup>2</sup> (El-Bihery, 2009; Lin et al., 2009; Simpson et al., 2010, among the others).

Within the above described framework, in this paper some improvements to the first version of the groundwater flow model at regional scale are discussed. In particular, these novelties are related to the analysis of hydraulic head and of the hydrostratigraphic structure in those areas which appeared to be critical from the development of the first version of the model. More specifically, in some areas the thickness of the fresh water aquifer vanished and the aquifer appeared to be saturated with salt water through its whole thickness.

Moreover, since some input data of the model are estimated with high uncertainty, it is necessary to perform a sensitivity analysis in order to assess the reliability of the model predictions.

## Hydrostratigraphy of the study area

The Salento carbonatic continental shelf is part of the Apulian foreland which was created during the Apenninic orogenesis and corresponded to a wide antiformal structure, WNW–ESE trending, block-faulted, and was variably uplifted during late neogenic times following the geotectonic events that have affected the whole Mediterranean area.

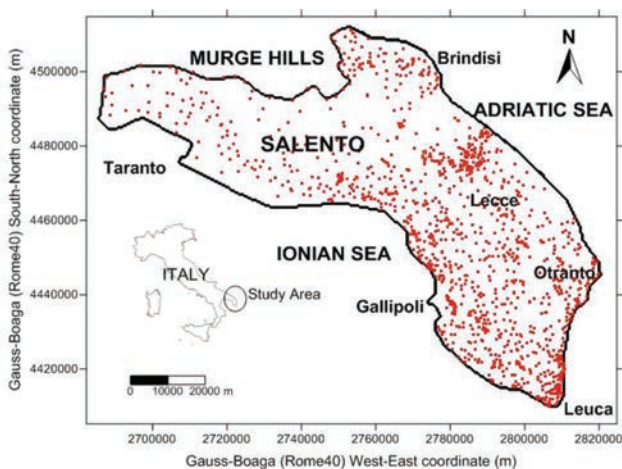


Fig. 1 - Location of Salento peninsula. The red dots indicate the location of the wells used for the construction of the conceptual model.

Fig. 1 - Localizzazione della penisola Salentina. I punti rossi indicano la posizione dei pozzi utilizzati per la costruzione del modello concettuale.

The rocks of Salento were subjected to karst processes that modeled them, when the region suffered periodic emergences because of tectonic or climatic causes. During these times, in fact, natural waters flowing on the surface could infiltrate into the ground through the dense network of fractures, cracks or bedding planes present in the limestone, stretching it more and more. For its karst nature, the study area has few surface water resources but, on the contrary, has considerable groundwater resources, thanks to the presence of a multilayer aquifer system. The groundwater is mainly hosted in limestone formations, dating back to the period between the Cretaceous and the Oligocene. More superficial semi-confined aquifers are hosted in formations that date back to the Miocene, the Pliocene and the Pleistocene. These shallow aquifers are limited in size and thickness, so they are less important at the regional scale than the main aquifer. Therefore water resources mainly consist of the groundwater contained in the Cretaceous carbonate aquifer, in some quite permeable levels in the Miocene deposits and in a coastal shallow aquifer hosted by the Plio-Pleistocene deposits and partly connected with the deep aquifer. Water circulates in the carbonate aquifer through karst conduits and fractures, whereas groundwater flow in Miocene and Plio-Pleistocene deposits seems to be controlled by the porosity of the rocks. The deep aquifer and some shallow aquifers are of coastal type, since fresh groundwater is sustained at the base by seawater.

The analysis of the complex stratigraphic architecture of the region and the relationship between the deep coastal aquifer and the sea are fundamental for the development of a model which can properly simulate groundwater flow.

The hydrostratigraphic model of the Salento peninsula is supported by the description of different geological formations (Margiotta and Negri, 2004) and by the analysis of lithologic data from more than 1000 boreholes, scattered in the study area (Fig.1). According to this model, it is possible to recognize seven hydrostratigraphic units (Giudici et al., 2012a; De Filippis, 2012), which are briefly described below and some of which include several lithostratigraphic units. The boundary surfaces between hydrostratigraphic units were obtained by interpolation of the well-data and with the help of two-dimensional geological sections for further checks. For details about the zones where these formations outcrop and their thicknesses, see the maps by Giudici et al. (2012a).

The oldest hydrostratigraphic unit (Calcare di Altamura – Altamura limestone) hosts the deep aquifer of the peninsula and consists of fractured limestone and dolomitic limestone, dating back between the Cretaceous and the Oligocene. This hydrostratigraphic unit reaches about 5600 m in depth below ground surface, while its top varies from 250 m above the mean sea level in the northwestern side of the area, to 200 m below the mean sea level near Lecce, to 100 m below the mean sea level near Brindisi and down to 250 m below the mean sea level near Taranto (Fig.2). The interface between fresh water and salt water lays inside this unit and extends inland.

The hydrostratigraphic unit corresponding to the Galatone

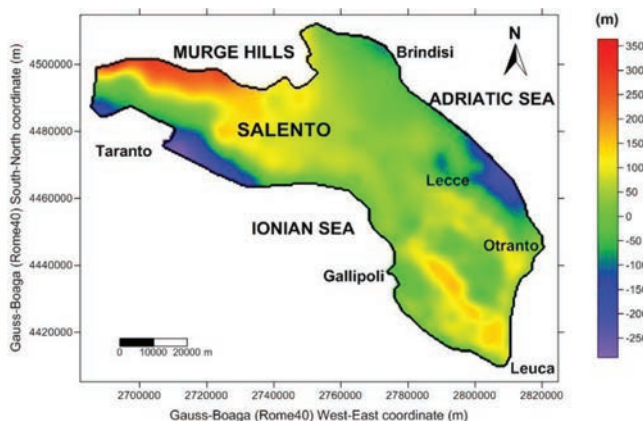


Fig. 2 - Top level of the hydrostratigraphic unit corresponding to Altamura limestone.

Fig. 2 - Quota del tetto dell'unità idrostratigrafica corrispondente al Calcare di Altamura.

formation dates back to the Oligocene and is present both along the coast and inland. This unit consists of fine-grained and very compact limestones, marls and deposits of sandy clays. It reaches a maximum thickness of 70 m.

The hydrostratigraphic unit dating back to the Miocene consists of calcarenites and is present in a wide area corresponding the eastern and south-central part of Salento. It hosts underground water bodies where porous deposits rest on very poorly permeable, marly or clayey, sediments. The thickness of this hydrostratigraphic unit exceeds 150 m in correspondence of the eastern side of the peninsula.

The hydrostratigraphic unit dating back to the Pliocene is characterized by poorly permeable detrital rocks, which may present permeable intervals that would lead to the formation of relatively shallow underground water bodies. These rocks outcrop in a narrow strip near the Adriatic sea and their maximum thickness is about 100 m.

The hydrostratigraphic unit dating back to the early Pleistocene, corresponding to the formation of Gravina calcarenites, is widely outcropping in the study area. It is characterized by coarse-grained calcarenites and contains shallow aquifers with limited extension. It reaches a maximum thickness of almost 80 m near Lecce.

The hydrostratigraphic unit dating back to the middle-lower Pleistocene corresponds to the lithostratigraphic unit of the poorly permeable subappennine clays. The thickness of this unit increases towards the west coast, where it reaches a maximum of 230 m in the Taranto area. More modest thicknesses (up to 50 m) are observed in the province of Brindisi and in the central-western Salento.

The hydrostratigraphic unit dating back to the late Pleistocene is located in correspondence of the Brindisi-Taranto plain and along the western part of the peninsula. It is characterized by coarse-grained calcarenitic deposits (terrace deposits) and by fine-grained sand, silt and clay deposits along Brindisi coast (Brindisi sands). The thickness of this unit reaches up to 40 m to the south of Brindisi and lower values in other areas.

The previous hydrostratigraphic unit hosts superficial po-

rous aquifers, covered by recent continental deposits with low permeability. The sediments of this unit have small thicknesses (a few meters) in the Taranto area and higher thicknesses (about 10 m) in the Brindisi area.

### Revision of the conceptual model

The results of Giudici et al. (2012a) showed that some portions of the aquifer could be fully saturated with salt water. This is a very important result, that might have great relevance if the aim of the numerical model is to provide a tool to support decisions that limit and possibly prevent the salinization and desertification phenomena. Moreover, under these conditions, the non-linearity of the numerical model might cause difficulties to the solution of the forward problem and therefore uncertainties on the model outcomes.

As a consequence, a revision of the conceptual model has been carried on, in order to make the model results even more reliable. Such a revision mainly involves the reference piezometric head and the top of the deep aquifer, as discussed below.

The content of the fresh water stored in the aquifer is estimated from the thickness of the freshwater aquifer ( $\theta$ ), which can be given by:

$$\theta = \min(t; h) - (-\delta h) = \min(t; h) + \delta h = \begin{cases} t + \delta h & \text{if } h > t \\ (1 + \delta)h & \text{if } h \leq t \end{cases} \quad (1)$$

where  $h$  is the piezometric head,  $t$  is the top of Altamura limestone (Fig.2) with respect to the mean sea level,  $\delta$  depends on the densities of fresh water and salt water, while  $(-\delta h)$  is the depth (below the mean sea level) of the interface between fresh water and salt water according to Ghyben-Herzberg approximation (Bear, 1979).

Using the  $h$  values (Fig.3) interpolated from well-data covering the whole area (Fig.1) and collected from 1954, but mostly in the last two decades, the  $t$  values shown in Fig.2 and the assumption that  $\delta=37$  (De Filippis, 2012), the map of  $\theta$  shown in Fig.4 is obtained. Notice that the piezometric level of the aquifer has suffered relatively small variations during the last 60 years, so that the use of data from a long period is justified to build a piezometric map; in fact, the plot of Fig.3 is similar to the piezometric maps of other authors (see, e.g., Regione Puglia, 2009). However, a little variation of  $h$  values induces a significant vertical shift of the interface between fresh and salt water, depending on the  $\delta$  value.

In the map of Fig.3, it can be easily noticed that  $\theta$  assumes negative values in the green to violet zones, where the aquifer is expected to be saturated with salt water. According to Eq. (1),  $\theta$  can assume negative values when:

- $h < 0$  m;
- $t < -\delta h$ , namely when the level of the interface between fresh water and salt water is higher than the top of Altamura limestone.

The former situation occurs in the red zones drawn in Fig.3. A detailed analysis of the piezometric data revealed some uncertain measurements, which were not coherent with the surrounding values and were related to wells that could be

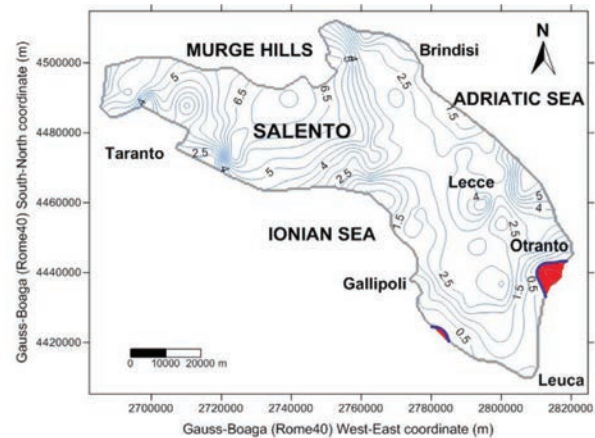


Fig. 3 - Contour map of the piezometric head over the whole study area (contour spacing: 0.5 m). Curves with  $h = 0$  m (blue curves) and zones with  $h < 0$  m (red zones) are evidenced.

Fig. 3 - Mappa della piezometria sull'intera regione in esame (curve equipiaziante di 0.5 m). Sono state evidenziate le isopieze con  $h = 0$  m (curve blu) e le zone con  $h < 0$  m (zone rosse).

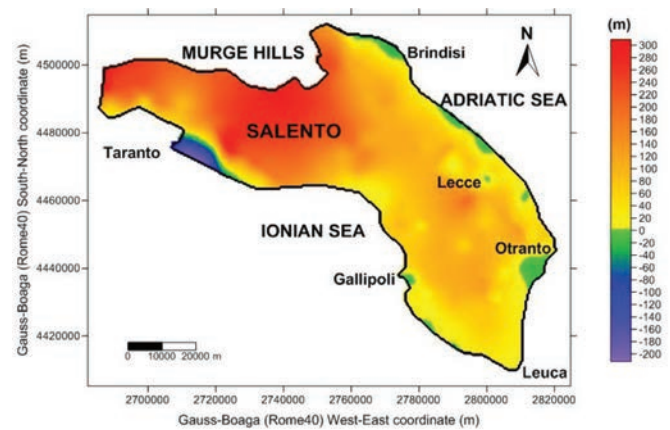


Fig. 4 - Thickness of the aquifer saturated with fresh water,  $\theta$ , over the whole study area.

Fig. 4 - Spessore della porzione dell'acquifero saturata da acqua dolce,  $\theta$ , sull'intera regione in esame.

drilled in shallow aquifers. Therefore, these data were considered inconsistent.

Moreover, two auxiliary points with  $h=0$  m were added near the west coast midway between Gallipoli and Leuca in order to reduce the extension of the zone where  $h < 0$  m, which corresponds to a green area in Fig.3, but is a mere effect of the data interpolation.

The hydraulic head interpolated after these modifications is assumed as the reference field for  $h$  and is used to reconstruct the groundwater flow direction in the deep aquifer of the Salento peninsula (Fig.5).

To point out the zones where  $t < -\delta h$ , twelve 2D hydrostratigraphic sections were drawn, partly with N-S direction and partly with W-E direction (Fig.6). From the 2D cross sections shown in Fig.7, the interface between fresh and salt water calculated by using Ghyben-Herzberg approximation appears to lay at a level higher than the top of the Altamura limestone in different zones. In such cases, if the Altamura limestone is in direct contact with the porous Gravina calcarenites, without the interposition of the impermeable sedi-

ments of the Galatone formation, it can be assumed that these hydrostratigraphic units exchange water and that the top of the deep aquifer coincides with the top of Gravina calcarenites. This situation clearly occurs near Brindisi (Fig.7c) and partly also south of Taranto, near Gallipoli and near Lecce. The differences between the top of the deep aquifer, reconstructed according to the criteria described above, and the top of the Altamura limestone are shown in Fig.8: they reach high values in some positions and, in particular, in the northern sector of the Salento, close to the border with the Murge, and with minor relevance along a strip from Gallipoli to Santa Maria di Leuca.

Using the modified values of  $h$  and  $t$  in Eq. (1), a revised map for  $\theta$  is obtained, as shown in Fig.9.

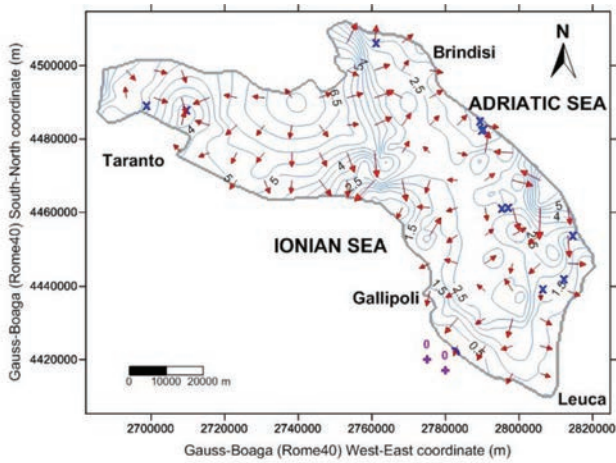


Fig. 5 - Piezometric data excluded (x) and added (+) after an analysis of  $h$  values for the wells scattered over the whole region. The contour map (contour spacing: 0.5 m) was obtained by interpolation of well data after this analysis. The arrows indicate the direction of groundwater flow in the aquifer system of Salento peninsula.

Fig. 5 - Dati di piezometria esclusi (x) e aggiunti (+) dopo un'analisi dei valori di  $h$  relativi ai pozzi sparsi sull'intera regione. Le curve di livello (equipacciate di 0.5 m) sono state ottenute per interpolazione dei dati di pozzo in seguito a tale analisi. Le frecce indicano la direzione del flusso delle acque sotterranee del sistema acquifero della penisola Salentina.

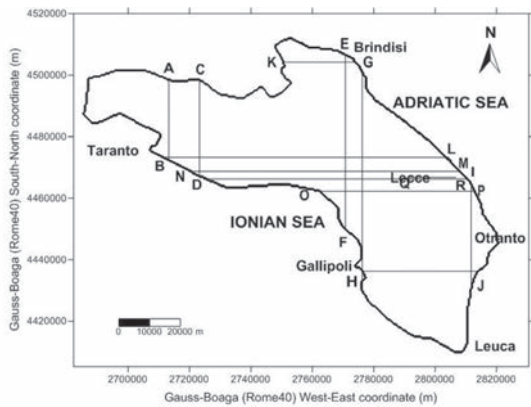


Fig. 6 - Location of the analysed hydrostratigraphic sections.

Fig. 6 - Ubicazione delle sezioni idrostratigrafiche analizzate.

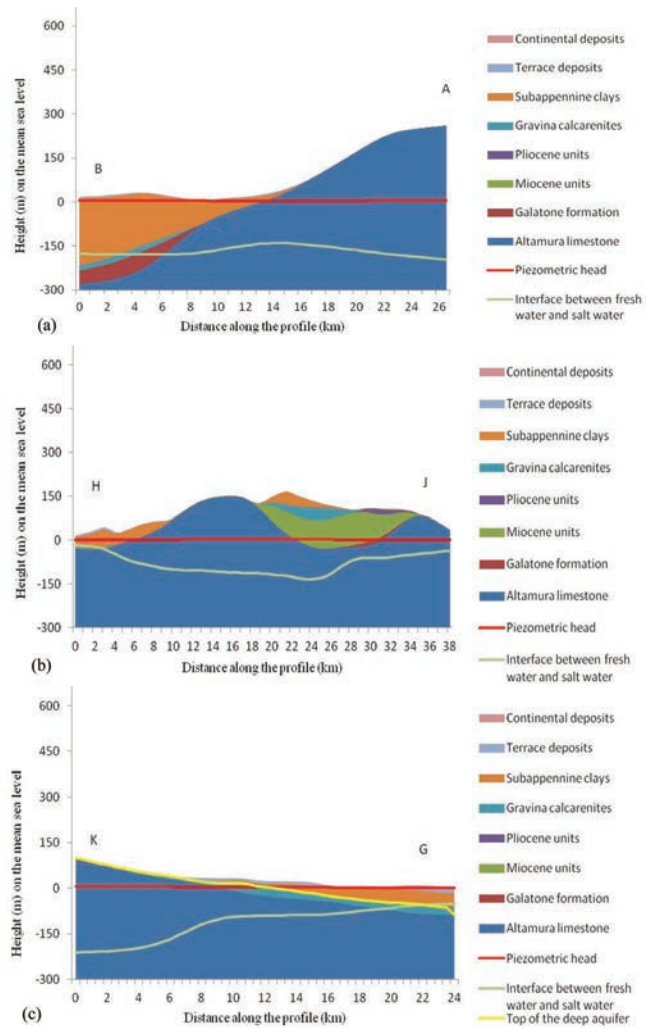


Fig. 7 - Hydrostratigraphic section AB and calculated interface between fresh and salt water (a). Hydrostratigraphic section HJ and calculated interface between fresh and salt water (b). Hydrostratigraphic section KG, calculated interface between fresh and salt water and location of deep aquifer's top (c).

Fig. 7 - Sezione idrostratigrafica AB e interfaccia acqua dolce-acqua salata calcolata (a). Sezione idrostratigrafica HJ e interfaccia acqua dolce-acqua salata calcolata (b). Sezione idrostratigrafica KG, interfaccia acqua dolce-acqua salata calcolata e posizione del tetto dell'acquifero profondo (c).

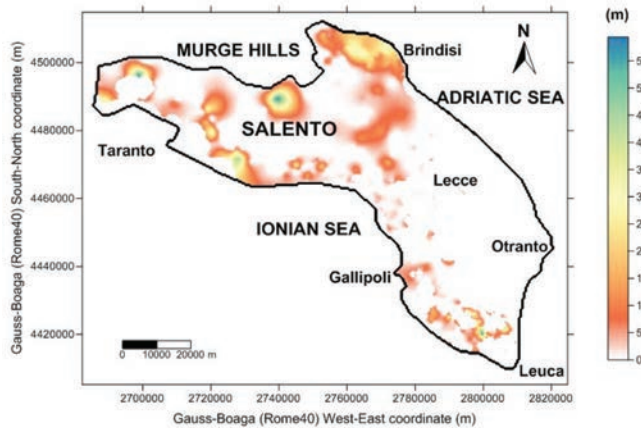


Fig. 8 - Difference between deep aquifer's top and Altamura limestone top.

Fig. 8 - Differenza tra le quote del tetto dell'acquifero profondo e del tetto del Calcere di Altamura.

Furthermore, the map of Fig.5 shows that the aquifer is mainly supplied from the Murge hills and discharges to the sea through both the Adriatic and Ionian coasts. Furthermore, one must take into account the recharge and the extraction terms through the development of a mathematical model.

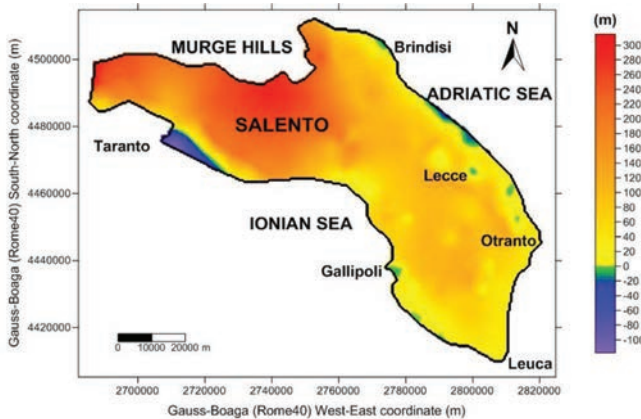


Fig. 9 -  $\theta$  values obtained after processing the piezometric data and after stratigraphic analysis of the areas where  $\theta < 0$  m.

Fig. 9 - Valori di  $\theta$  ottenuti dopo un'elaborazione delle piezometrie e dopo un'analisi stratigrafica delle aree in cui  $\theta < 0$  m.

## Mathematical model

The numerical model describing the groundwater flow in the karst aquifer of Salento is an evolution of the numerical code YAGMod (Yet Another Groundwater flow Model), developed by Cattaneo et al. (2012). It is implemented in Fortran90 and applies the method of finite differences to simulate hydraulic flow in porous or fractured media, under pseudo-steady flow conditions.

In this study, YAGMod was adapted to be used to solve the balance equation for a fluid moving in a saturated porous medium under pseudo-steady 2D flow conditions and when the bottom of the aquifer is characterized by the interface between fresh and salt water. As the model is based on the method of finite differences, the aquifer system is discretised with an appropriate regular grid in the horizontal plane. If each cell of the grid is denoted with the indices  $i$  and  $j$ , for each cell  $(i,j)$  the balance equation for two-dimensional pseudo-steady flow could be written as:

$$T_{(i+1/2;j)}(h_{(i+1;j)} - h_{(i;j)}) + T_{(i-1/2;j)}(h_{(i-1;j)} - h_{(i;j)}) + T_{(i;j+1/2)}(h_{(i;j+1)} - h_{(i;j)}) + T_{(i;j-1/2)}(h_{(i;j-1)} - h_{(i;j)}) = -F_{(i;j)} \quad (2)$$

where  $T_{(i\pm 1/2;j)}$  and  $T_{(i;j\pm 1/2)}$  are called internode transmittances and  $F_{(i;j)}$  is the source term in the cell  $(i,j)$ .

$T_{(i\pm 1/2;j)}$  and  $T_{(i;j\pm 1/2)}$  are related, in turn, to the internode hydraulic conductivities  $K_{(i\pm 1/2;j)}$  and  $K_{(i;j\pm 1/2)}$  and to the geometry of the grid and of the aquifer:

$$T_{(i\pm 1/2;j)} = K_{(i\pm 1/2;j)} \theta_{(i\pm 1/2;j)} \frac{\Delta x}{\Delta y}, \quad T_{(i;j\pm 1/2)} = K_{(i;j\pm 1/2)} \theta_{(i;j\pm 1/2)} \frac{\Delta y}{\Delta x}$$

where  $\Delta x$  and  $\Delta y$  are the side lengths of the cell along the  $x$  and  $y$  axes, respectively, and

$$\theta_{(i\pm 1/2;j)} = \frac{\theta_{(i;j)} + \theta_{(i\pm 1;j)}}{2}, \quad \theta_{(i;j\pm 1/2)} = \frac{\theta_{(i;j)} + \theta_{(i;j\pm 1)}}{2}$$

represent the arithmetic averages of the saturated thickness of two adjacent cells. Specifically,  $\theta_{(i;j)}$  is the saturated thickness of the cell  $(i,j)$  and is defined as:

$$\theta_{(i;j)} = \begin{cases} \Delta z_{(i;j)} & \text{if } h_{(i;j)} > \text{top}_{(i;j)} \\ h_{(i;j)} - \text{bot}_{(i;j)} & \text{if } \text{bot}_{(i;j)} < h_{(i;j)} \leq \text{top}_{(i;j)} \\ 0 & \text{if } h_{(i;j)} \leq \text{bot}_{(i;j)} \end{cases} \quad (3)$$

where  $\text{top}_{(i;j)}$  and  $\text{bot}_{(i;j)}$  represent the levels of the top and of the bottom of the cell  $(i,j)$ , respectively, while  $\Delta z_{(i;j)} = \text{top}_{(i;j)} - \text{bot}_{(i;j)}$ . Notice that the Cretaceous and Oligocene formations which host the aquifer under study are so thick that the bottom of each cell corresponds to the level of the fresh/salt water interface and the third condition of Eq. (3) is never verified. Therefore Eq. (3) corresponds to its continuous counterpart, Eq. (1), if  $\text{top}_{(i;j)}$  is replaced with  $t$  and  $\text{bot}_{(i;j)}$  with  $(-\delta h)$ .

YAGMod accounts for different types of source terms and boundary conditions. In fact, it can consider distributed or punctual source terms. Furthermore, it handles both fixed source/sink terms, which are independent from the piezometric level, and variable source terms, which depend on the water head, as, for instance, a drain or river-aquifer interaction.

If Eq. (2) is written for each cell of the domain, a system of non-linear algebraic equations is obtained. This system could be solved using the over-relaxation iterative method, whose approximate solution at the  $l$ -th iteration is obtained at each node, firstly by computing the estimate with the classic method of Gauss-Seidel,  $h_{(i;j)}^{(l)}$ , and then by weighting the correction with respect to the previous iteration,  $h_{(i;j)}^{(l-1)}$ , by a relaxation parameter  $1 < \omega < 2$ :

$$h_{(i;j)}^{(l)} = h_{(i;j)}^{(l-1)} + \omega(h_{(i;j)}^{(*)} - h_{(i;j)}^{(l-1)}) = (1 - \omega)h_{(i;j)}^{(l-1)} + \omega h_{(i;j)}^{(*)}$$

## Boundary conditions

For the case study presented in this paper, we used a 2D computational grid with  $286 \times 220$  squared cells with 500 m side length. Along the boundary between the Salento peninsula and the Murge hills, Dirichlet boundary conditions were assigned, by using the reference piezometric level. Along the coasts, two types of boundary conditions were assigned:

- where the aquifer is under phreatic conditions ( $t > 0$  m), the outgoing flow from cells was modeled as a drain:

$$Q_{\text{drain}} = Ch, \quad (4)$$

where  $C$  is an appropriate conductance;

- where the aquifer is confined near the coast ( $t \leq 0$  m), the contact between Altamura limestone and the sea occurs offshore. Then, the estimate of the outgoing flow from

the border cells in these areas requires the knowledge of the aquifer characteristics until the contact point with the sea. This information would be available only thanks to costly marine geophysical surveys. Therefore a simpler strategy was chosen and Dirichlet boundary conditions were assigned by using the reference piezometric level.

In summary, Dirichlet boundary conditions were applied along the whole border of the domain, except for the cells along the coast where the aquifer is under phreatic conditions and a drainage term is introduced to simulate fresh water outflow toward the sea.

### Source terms

For the aquifer system presented in this paper, four source terms were recognized.

The rain infiltration through the thicknesses of the hydrostratigraphic units is a distributed and fixed recharge term. In this case, the flow rate on the whole peninsula could be estimated as:

$$q_{rec} = P C_{inf} \quad (5)$$

where  $P$  (mm/year) is the flow rate per unit surface obtained by interpolating the annual rainfall from 1921 to 1999, measured in 20 meteorological stations managed by the Ufficio Idrografico e Mareografico in Bari, while  $C_{inf}$  is called infiltration coefficient and is calculated as a weighted harmonic mean of the thicknesses of the hydrostratigraphic units. The weights used for this aim take into account the hydraulic behavior of the sediments and are higher for more permeable sediments.

A constant flow rate ( $10^{-3} \text{ m}^3 \text{ s}^{-1}$ ) was assigned where sinkholes and dolines are found. This is a punctual and fixed recharge term and occurs in 99 locations in the study area, where these karst manifestations are present.

The extractions for agricultural purposes were classified according to the soil use on the whole area. We assumed the following extracted flow rates per cell for the irrigation of four kinds of crops:

- $3.17 \times 10^{-3} \text{ m}^3 \text{ s}^{-1}$  for vineyards;
- $3.96 \times 10^{-5} \text{ m}^3 \text{ s}^{-1}$  for olive trees;
- $3.17 \times 10^{-5} \text{ m}^3 \text{ s}^{-1}$  for land used for other crops;
- $7.93 \times 10^{-6} \text{ m}^3 \text{ s}^{-1}$  for green urban areas.

The extracted flow rates per cell for drinking purposes were estimated by dividing the peninsula into three sub-areas (Regione Puglia 2009):

- $2.9 \times 10^{-4} \text{ m}^3 \text{ s}^{-1}$  for the province of Brindisi;
- $2.4 \times 10^{-2} \text{ m}^3 \text{ s}^{-1}$  for the Ionic side;
- $3.7 \times 10^{-2} \text{ m}^3 \text{ s}^{-1}$  for the Adriatic side.

### Model calibration

YAGMod includes a module for the model calibration with the CMM, the Comparison Model Method (Scarascia and Ponzini, 1972; Ponzini and Lozej, 1982; Ponzini and Crosta, 1988), by determining the conductivity field for 2D and stationary flows through the solution of an inverse problem. This

method requires (i) the knowledge of the reference piezometric head field ( $h^{(ref)}$ ) (Fig.5), which is obtained by interpolating well-data and filtering the result to limit the effect of the instability on the inversion due to the components with high wavenumbers of the  $h^{(ref)}$  field (Giudici and Vassena, 2008), (ii) an estimate of a reference source term and (iii) an initial estimate of the conductivity field ( $K^{(CM)}$ ). Using these estimates and the  $h^{(ref)}$  field for Dirichlet boundary conditions, one can solve the balance equation obtaining the piezometric head field ( $h^{(CM)}$ ).

Then, the water discharge flowing through the aquifer thickness per unit horizontal length could be calculated for each cell as:

$$Q_{(i;j)}^{(CM)} = -K_{(i;j)}^{(CM)} \theta_{(i;j)}^{(CM)} \nabla h_{(i;j)}^{(CM)} \quad (6)$$

where  $\theta^{(CM)}$  is the saturated thickness of the aquifer calculated using  $h^{(CM)}$  field, while  $\nabla h_{(i;j)}^{(CM)}$  is obtained using the centered differences.

If  $h^{(ref)}$  is a good approximation of the real piezometric head field, the real hydraulic flux could be estimated as:

$$Q_{(i;j)} = -K_{(i;j)} \theta_{(i;j)}^{(ref)} \nabla h_{(i;j)}^{(ref)} \quad (7)$$

where  $\theta^{(ref)}$  is the saturated thickness of the aquifer calculated using  $h^{(ref)}$  field and  $K_{(i;j)}$  is the real conductivity field.

If  $K^{(CM)}$  is a good approximation of the real conductivity field, one could assume that  $Q_{(i;j)}^{(CM)} \approx Q_{(i;j)}$ . By considering the absolute value of the quantities appearing in Eq. (6) and Eq. (7), an estimate of the conductivity field can be obtained by using the integral approach of the CMM:

$$K^{(est)} = K^{(CM)} \frac{\theta^{(CM)} \left| \nabla h^{(CM)} \right|}{\theta^{(ref)} \left| \nabla h^{(ref)} \right|} \quad (8)$$

For this case study, a constant value for  $K^{(CM)}$  (homogeneous medium) was considered. In particular, different values for  $K^{(CM)}$  and  $C$  – see Eq. (4) – were tested to find the optimal couple of parameters which minimizes the mean absolute error, the mean square error and the maximum error on the  $h^{(CM)}$  field and on the piezometric head field calculated thanks to the balance equation with respect to the reference piezometric head. A series of tests have shown that the errors on the estimate of the piezometric head are not very sensible to variations of the  $C$  parameter. In fact, the mean absolute error on the piezometric head obtained as the solution of the balance equation, compared to the reference piezometric head, is shown for different values of  $K$  and  $C$  in Fig.10 and one could notice that there are not significant variations of these errors along the  $C$  axis. As a result of this analysis, the couple  $K^{(CM)} = 3 \times 10^{-3} \text{ m s}^{-1}$ ,  $C = 3 \times 10^{-2} \text{ m}^2 \text{ s}^{-1}$  was chosen since it minimizes the errors on the estimate of the piezometric level, but also by taking into account that, comparing the model results, the error on the global balance of the aquifer increases in correspondence of an increase of  $K^{(CM)}$ . By using this value

for  $K^{(CM)}$  in Eq. (8), the conductivity field shown in Fig.11 was identified.

In order to assess the improvement of the model fit obtained with the CMM, the maps of the differences between the modeled piezometric head and  $h^{(ref)}$  are shown in Fig.12, both for the homogeneous medium (Fig.12a) and for the conductivity field shown in Fig.11 (Fig.12b). These maps show that the ho-

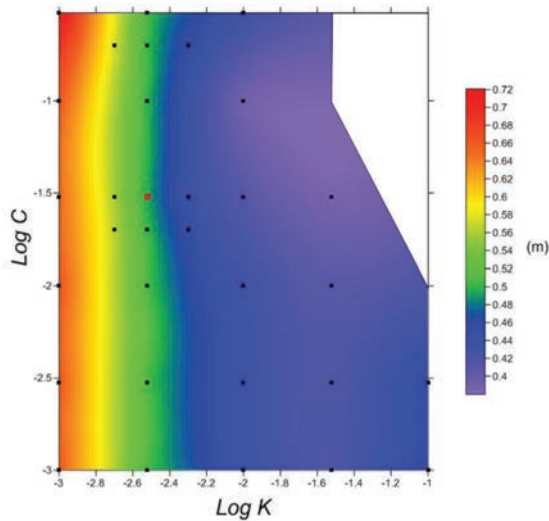


Fig. 10 - Mean absolute error on the piezometric level obtained as the solution of the balance equation, compared to the reference piezometric head, for different values of  $K$  and  $C$ . The points correspond to different pairs  $(K, C)$  for which the tests were performed. The white area corresponds to pairs of values that do not allow the convergence of the algorithm.

Fig. 10 - Errore medio assoluto sull'altezza piezometrica ottenuta come soluzione dell'equazione di bilancio, rispetto a quella di riferimento, per diversi valori di  $K$  e  $C$ . I punti corrispondono alle diverse coppie  $(K, C)$  per cui sono state eseguite le prove. La zona bianca corrisponde a coppie di valori che non permettono la convergenza dell'algoritmo.

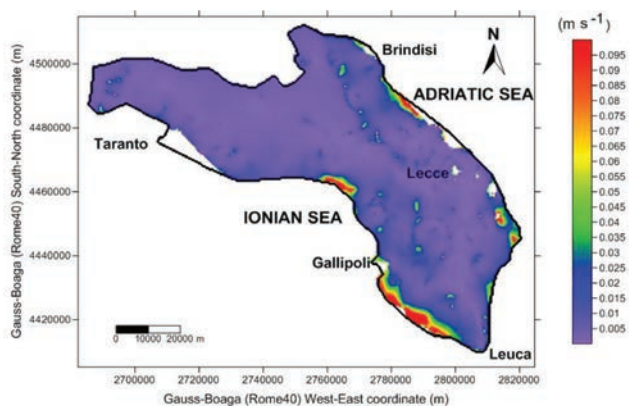


Fig. 11 - Hydraulic conductivity estimated by the application of CMM for the heterogeneous medium. The white areas refer to cells in which the thickness of the aquifer ( $\theta$ ) is negative: in these cells a no flow condition was assigned, in order to ensure the convergence of the algorithm

Fig. 11 - Conducibilità idraulica stimata in seguito all'applicazione del CMM per il mezzo eterogeneo. Le zone bianche si riferiscono alle celle in cui lo spessore dell'acquifero ( $\theta$ ) è negativo: a tali celle è stata assegnata una condizione di flusso nullo, al fine di garantire la convergenza dell'algoritmo.

mogeneous medium approximation is too drastic for the case study, with a maximum error close to 6 m (Fig.12a). On the other hand the piezometric head simulated for the heterogeneous medium after the application of the CMM differs from the  $h^{(ref)}$  field at most by about 2 m (Fig.12b).

## Model results

The balance terms for the heterogeneous medium are listed in Tab.1, while the flow direction obtained solving the balance equation into the whole domain is shown in Fig.13. These results confirm the qualitative remarks from the conceptual model: the flow through the boundary between the Salento peninsula and the Murge hills is mainly incoming, while that through the coasts is generally outgoing. The incoming flow through the Adriatic coast is due to the presence of a south-eastern zone with high  $h$  values, while that through the Ionian coast is due to its complex geometry.

Furthermore, the main recharge term of the aquifer is re-

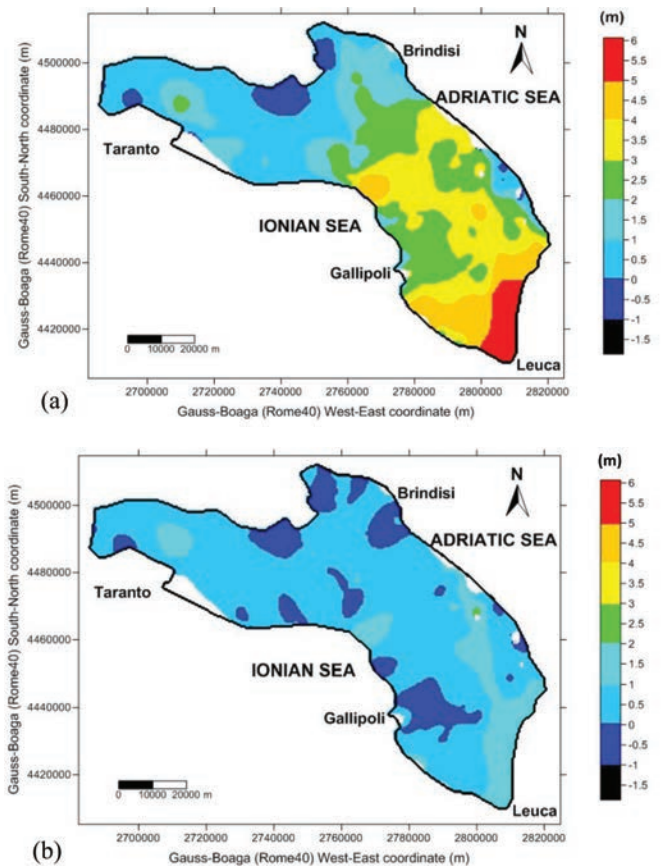


Fig. 12 - Difference between the piezometric head estimated for the homogeneous medium and the reference piezometric head (a) and between the piezometric head estimated for the heterogeneous medium and the reference piezometric head (b). The white areas refer to cells in which the thickness of the aquifer ( $\theta$ ) is negative: in these cells a no flow condition was assigned, in order to ensure the convergence of the algorithm.

Fig. 12 - Differenza tra l'altezza piezometrica stimata con il mezzo omogeneo e l'altezza piezometrica di riferimento (a) e tra l'altezza piezometrica stimata con il mezzo eterogeneo e l'altezza piezometrica di riferimento (b). Le zone bianche si riferiscono alle celle in cui lo spessore dell'acquifero ( $\theta$ ) è negativo: a tali celle è stata assegnata una condizione di flusso nullo, al fine di garantire la convergenza dell'algoritmo.

lated to rain infiltration, while the recharge due to sinkholes and dolines is irrelevant. Finally, withdrawals are mainly due to agricultural uses: on the other hand, the extractions for industrial purposes mainly affect the shallow aquifer, which is not modeled in this study.

The simulation of the discharge through submarine and subaerial sources, which are very important especially in the Taranto area, is included in the outgoing fluxes toward the sea along the coastal boundaries. This is a rough approximation, as these drainage terms for the aquifer could be highly influenced by local conditions. However, the hydrostratigraphic situation along the coast where these sources are most relevant, as in the Taranto gulf, is very complex, as shown by Fig.7a and, at the authors' knowledge, recent direct measurements of the discharge of these sources are missing.

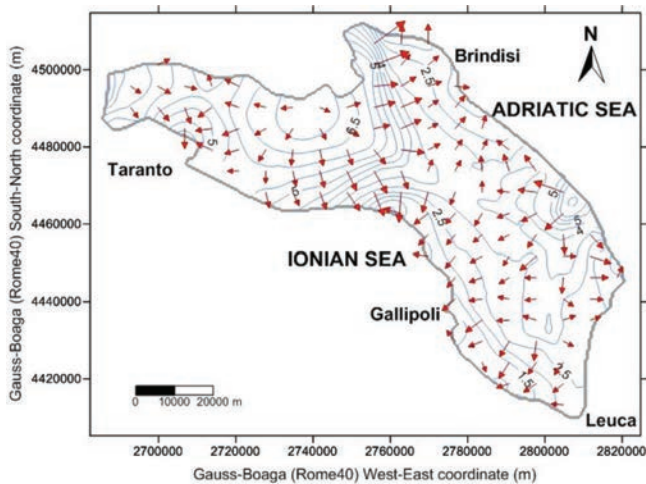


Fig. 13 - Direction of groundwater flow in the aquifer system of Salento peninsula. The curves (contour spacing: 0.5 m) represent the piezometric head estimated for the heterogeneous medium.

Fig. 13 - Direzione del flusso delle acque sotterranee del sistema acquifero della penisola Salentina. Le curve (equispaziate di 0.5 m) rappresentano l'altezza piezometrica stimata con il mezzo eterogeneo.

Tab. 1 - Balance terms for the heterogeneous medium.

Tab. 1 - Termini di bilancio per il mezzo eterogeneo.

Balance terms	Incoming flow ( $\text{m}^3 \text{s}^{-1}$ )	Outgoing flow ( $\text{m}^3 \text{s}^{-1}$ )
Flow through the boundary between the Salento peninsula and the Murge hills	4.7	-3.1
Flow through the coast:		
• Ionian coast (confined aquifer)	0.5	-14.9
• Adriatic coast (confined aquifer)	0.4	-6.6
• Ionian and Adriatic coasts (aquifer under phreatic conditions)	0	-8.4
Recharge due to rain infiltration	58.2	0
Recharge due to sinkholes and dolines	0.1	0
Withdrawals for drinking purposes	0	-3.3
Withdrawals for agricultural uses	0	-30.2

## Sensitivity analysis

Even after the calibration of a mathematical model, some input parameters are affected by some uncertainty, which reflects itself on the model results. Moreover, the non linearity of studied physical processes makes it difficult to identify which parameters have to be known with a higher accuracy to obtain physically consistent results and more realistic predictions. In this context, a sensitivity analysis could quantify the reliability of model's predictions and identify which parameters require a better estimate (Saltelli et al., 2008; Hill and Tiedemann, 2006).

For the case study, a sensitivity analysis was conducted following the approach proposed by Baratelli et al. (2011) and Giudici et al. (2012b) for a highly non-linear model of the thermomechanical evolution of the Antarctic ice sheet and applied by Cattaneo et al. (2012) to an alluvial aquifer in Somaliland. The sensitivity indicators were analytically calculated by expressing a model output ( $Y$ ) as a second-order function of deviations ( $\Delta x_i$ ,  $i=1, \dots, n$ ) of some input parameters ( $X_i$ ,  $i=1, \dots, n$ ) from their reference values ( $x_{i,ref}$ ,  $i=1, \dots, n$ ):

$$Y = g(\mathbf{X}) = y_{ref} + \mathbf{J} \cdot (\mathbf{X} - \mathbf{x}_{ref}) + 1/2 (\mathbf{X} - \mathbf{x}_{ref})^t \mathbf{H} (\mathbf{X} - \mathbf{x}_{ref}),$$

where  $y_{ref} = g(\mathbf{x}_{ref})$ ,  $\mathbf{X} = (X_1, \dots, X_n)^t$ ,  $\mathbf{x}_{ref} = (x_{1,ref}, \dots, x_{n,ref})^t$ , while  $\mathbf{J}$  vector and  $\mathbf{H}$  matrix are the gradient and the hessian matrix, respectively, of the  $g$  function, both evaluated in  $\mathbf{x}_{ref}$ .

Three sensitivity indicators were calculated:

- the prediction scaled sensitivity, which takes into account the relative variation of  $Y$  corresponding to a relative variation of a parameter  $X_i$ :

$$pss_i = \frac{dY}{y_{ref}} \frac{x_{i,ref}}{dX_i}$$

- the normalized dimensionless sensitivity, which takes into account the variability of  $X_i$  and  $Y$  through their standard deviations ( $\sigma_i$  and  $\sigma_Y$ , respectively):

$$S_i^\sigma = \frac{\sigma_i}{\sigma_Y} \frac{\partial g}{\partial X_i} (x_{ref})$$

- the first order sensitivity index, which is based on the variance of the model output and takes into account the whole variability of input parameters:

$$S_i = \frac{\text{var}_{X_i} [E_{X_{-i}} [Y | X_i]]}{\sigma_Y^2}$$

where  $E_{X_{-i}} [Y | X_i]$  is the expected value of model's output, conditioned on the  $X_i$  parameter, namely by considering the variation of all input parameters except for  $X_i$  (which is fixed), and  $\text{var}_{X_i}$  is the variance with respect to the variability of  $X_i$ .

Notice that, from the definition of  $\mathbf{J}$ ,  $S_i^\sigma = \sigma_i \sigma_Y^{-1} J_i$  and  $pss_i = x_{i,ref} y_{ref}^{-1} J_i$ . These are local indexes, as they take into account the linear approximation of the model only and neglect non linear effects, while  $S_i$  allows to overcome these lim-

its, because it accounts for the whole variability of the independent variables.

The indicators  $S_i^\sigma$ ,  $ps_s$  and  $S_i$  were calculated for the following output parameters:

- the mean absolute error, the mean square error and the maximum error of the  $h^{(CM)}$  field with respect to the reference piezometric head;
- the mean absolute error, the mean square error and the maximum error on the piezometric head field calculated from the balance equation with respect to the reference piezometric head;
- the incoming and outgoing fluxes through the boundary between Salento and the Murge hills;
- the incoming and outgoing fluxes through the coasts;
- the outgoing flux through cells where the aquifer is under phreatic conditions;
- the volume of aquifer saturated with fresh water;
- the mean value of  $K^{(est)}$  (see Eq. (8)) and of  $\log(K^{(est)})$  and their variances.

The following input parameters have been analyzed:

- $\log(K^{(CM)})$  (see Eq. (8));
- the recharge term of the aquifer due to rain infiltration, namely the parameter P in Eq. (5);
- the weights used to calculate  $C_{inf}$ ;
- the extracted flow rates for irrigation and for drinking purposes;
- the recharge term due to sinkholes and dolines;
- the conductance C (see Eq. (4));
- the parameter  $\delta$  (see Eq. (1)).

For each of these parameters a variation  $\Delta x_i = \pm 0.2 x_{i,ref}$  was considered, except for rain infiltration to which was applied a variation  $\Delta x_i = \pm 0.1 x_{i,ref}$  because of convergence problems of the iterative solution of the forward problem for higher variations.

The obtained results (Fig.14) show that the most sensitive output parameters are the flow terms through the domain boundary and the volume of the aquifer. In particular, a variation of  $\log(K^{(CM)})$  could induce significant variations on the

pss		Coefficients for eff.infiltration											Water abstraction										
		Log $K^{(CM)}$	Rain	Cretaceous	Dolomite	Miocene	Pliocene	Lower Pleistocene	Lower to Middle Pleistocene	Upper Pleistocene	Vineyards	Agricultural land	Drove production	Urban areas	Drinkable purposes	Recharge through dolines	Conductance of drainage BCs	$\delta$					
Errors on $h^{(est)}$	Aver.Abs.error	-1.59	0.87	0.82	0.05	0.30	0.03	0.07	0.17	0.02	-0.88	0.00	-0.01	0.00	-0.16	0.00	0.06	-1.37					
	RMS error	-1.55	0.80	0.77	0.05	0.30	0.03	0.06	0.13	0.02	-0.79	0.00	0.00	0.00	-0.16	0.00	0.00	-1.27					
	Maximum error	-1.64	0.44	0.50	0.04	0.10	0.01	0.02	0.04	0.00	-0.37	0.00	0.00	0.00	-0.07	0.00	0.31	-0.86					
Flow rates through the boundaries	Aver.Abs.error	-0.62	0.76	0.64	0.05	0.35	0.02	0.07	0.15	0.01	-0.88	0.00	-0.01	0.00	-0.19	0.00	-0.04	-0.55					
	RMS error	-0.87	1.26	1.05	0.10	0.73	0.05	0.12	0.19	0.03	-0.48	0.00	-0.01	0.00	-0.39	0.01	-0.59	-0.70					
	Maximum error	-0.39	0.60	0.33	0.10	0.53	0.03	0.07	0.09	0.03	-0.73	0.00	-0.01	0.00	-0.20	0.00	0.00	-0.11					
Fresh water aquifer volume	Aver.Abs.error	-0.74	-0.44	-0.55	0.00	0.00	0.00	-0.05	-0.13	-0.02	-0.58	0.00	0.00	0.00	0.01	0.00	1.02	0.47					
	RMS error	0.76	0.85	1.04	0.00	0.00	0.00	0.06	0.13	0.02	-1.03	0.00	0.00	0.00	-0.01	0.00	0.95	1.14					
	Maximum error	1.30	0.07	0.08	0.00	0.01	0.00	0.00	0.01	0.00	0.09	0.00	0.00	0.00	0.01	0.00	1.05	-0.03					
Statistics of $K^{(est)}$	Average $K$	0.26	0.68	0.64	0.05	0.23	0.02	0.06	0.10	0.01	-0.64	0.00	0.00	0.00	-0.11	0.00	0.09	-0.87					
	Variance $K$	0.04	0.98	0.97	0.08	0.31	0.03	0.08	0.18	0.01	-0.96	0.00	-0.01	0.00	-0.17	0.01	0.14	-1.26					
	Average Log $K$	-0.13	-0.09	-0.08	-0.01	-0.04	0.00	-0.01	0.00	0.00	0.08	0.00	0.00	0.00	0.01	0.00	-0.01	0.11					
Flow rates through the boundaries	Average Log $K$	-0.29	-0.16	-0.13	-0.02	-0.08	0.00	-0.02	0.00	0.00	0.13	0.00	0.00	0.00	0.02	0.00	-0.02	0.19					

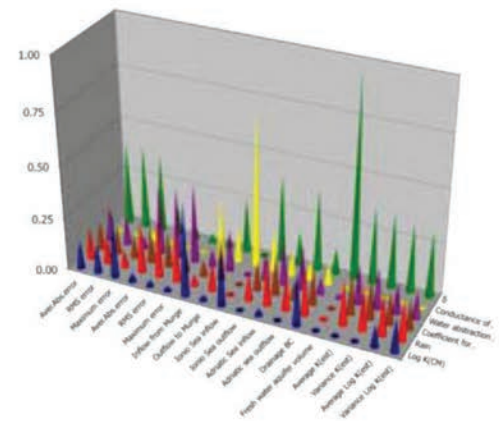
(a)

$S_i$		Coefficients for eff.infiltration											Water abstraction										
		Log $K^{(CM)}$	Rain	Cretaceous	Dolomite	Miocene	Pliocene	Lower Pleistocene	Lower to Middle Pleistocene	Upper Pleistocene	Vineyards	Agricultural land	Drove production	Urban areas	Drinkable purposes	Recharge through dolines	Conductance of drainage BCs	$\delta$					
Errors on $h^{(est)}$	Aver.Abs.error	0.13	0.15	0.14	0.00	0.02	0.00	0.00	0.01	0.00	0.16	0.00	0.00	0.00	0.00	0.00	0.00	0.39					
	RMS error	0.14	0.15	0.14	0.00	0.02	0.00	0.00	0.00	0.00	0.14	0.00	0.00	0.00	0.00	0.00	0.00	0.39					
	Maximum error	0.31	0.09	0.12	0.00	0.00	0.00	0.00	0.00	0.00	0.06	0.00	0.00	0.00	0.00	0.00	0.00	0.37					
Flow rates through the boundaries	Aver.Abs.error	0.04	0.24	0.17	0.00	0.05	0.00	0.00	0.01	0.00	0.33	0.00	0.00	0.00	0.00	0.00	0.00	0.13					
	RMS error	0.03	0.26	0.17	0.00	0.09	0.00	0.00	0.01	0.00	0.34	0.00	0.00	0.00	0.00	0.00	0.00	0.08					
	Maximum error	0.02	0.23	0.09	0.01	0.14	0.00	0.00	0.00	0.00	0.38	0.00	0.00	0.00	0.00	0.00	0.00	0.05					
Fresh water aquifer volume	Aver.Abs.error	0.44	0.05	0.08	0.00	0.00	0.00	0.00	0.00	0.00	0.08	0.00	0.00	0.00	0.00	0.00	0.00	0.26					
	RMS error	0.03	0.14	0.21	0.00	0.00	0.00	0.00	0.00	0.00	0.20	0.00	0.00	0.00	0.00	0.00	0.00	0.25					
	Maximum error	0.00	0.00	0.00	0.00	0.00	0.00	0.00	0.00	0.00	0.01	0.00	0.00	0.00	0.00	0.00	0.00	0.00					
Statistics of $K^{(est)}$	Average $K$	0.01	0.21	0.19	0.00	0.03	0.00	0.00	0.01	0.00	0.20	0.00	0.00	0.00	0.00	0.00	0.00	0.36					
	Variance $K$	0.00	0.21	0.20	0.00	0.02	0.00	0.00	0.01	0.00	0.20	0.00	0.00	0.00	0.00	0.00	0.00	0.35					
	Average Log $K$	0.11	0.20	0.16	0.00	0.04	0.00	0.00	0.00	0.00	0.15	0.00	0.00	0.00	0.00	0.00	0.00	0.31					
Flow rates through the boundaries	Variance Log $K$	0.16	0.19	0.14	0.00	0.05	0.00	0.00	0.00	0.00	0.13	0.00	0.00	0.00	0.00	0.00	0.00	0.33					

(b)

$S_i^\sigma$		Coefficients for eff.infiltration											Water abstraction										
		Log $K^{(CM)}$	Rain	Cretaceous	Dolomite	Miocene	Pliocene	Lower Pleistocene	Lower to Middle Pleistocene	Upper Pleistocene	Vineyards	Agricultural land	Drove production	Urban areas	Drinkable purposes	Recharge through dolines	Conductance of drainage BCs	$\delta$					
Errors on $h^{(est)}$	Aver.Abs.error	-0.34	0.39	0.37	0.02	0.13	0.01	0.03	0.07	0.01	-0.40	0.00	0.00	0.00	0.03	0.00	0.03	-0.62					
	RMS error	-0.35	0.39	0.37	0.03	0.14	0.01	0.03	0.06	0.01	-0.38	0.00	0.00	0.00	-0.08	0.00	0.04	-0.61					
	Maximum error	-0.55	0.30	0.34	0.02	0.07	0.00	0.02	0.03	0.00	-0.25	0.00	0.00	0.00	-0.05	0.00	0.21	-0.58					
Flow rates through the boundaries	Aver.Abs.error	-0.20	0.49	0.42	0.03	0.23	0.01	0.04	0.09	0.01	-0.57	0.00	0.00	0.00	-0.13	0.00	-0.03	-0.36					
	RMS error	-0.17	0.51	0.42	0.04	0.29	0.02	0.05	0.08	0.01	-0.58	0.00	0.00	0.00	-0.15	0.00	-0.03	-0.28					
	Maximum error	-0.15	0.48	0.30	0.06	0.42	0.02	0.06	0.07	0.02	-0.62	0.00	-0.01	0.00	-0.16	0.00	0.00	-0.14					
Fresh water aquifer volume	Aver.Abs.error	0.67	-0.23	-0.28	0.00	0.00	0.00	-0.03	-0.07	-0.01	0.29	0.00	0.00	0.00	0.00	0.00	0.53	0.24					
	RMS error	-0.16	-0.37	-0.45	0.00	0.00	0.00	-0.03	-0.06	-0.01	0.45	0.00	0.00	0.00	0.00	0.00	-0.41	0.49					
	Maximum error	0.52	0.06	0.07	0.00	0.01	0.00	0.00	0.01	0.00	0.07	0.00	0.00	0.00	0.01	0.00	0.84	-0.03					
Statistics of $K^{(est)}$	Average $K$	-0.03	-0.36	-0.37	-0.02	-0.06	0.00	-0.03	-0.08	-0.01	0.35	0.00	0.00	0.00	0.05	0.00	-0.44	0.63					
	Variance $K$	-0.18	-0.40	-0.44	0.03	0.22	0.02	0.04	0.05	0.01	-0.46	0.00	0.00	0.00	-0.10	0.00	0.33	-0.38					
	Average Log $K$	-0.04	-0.41	-0.30	-0.02	-0.17	-0.03	-0.04	-0.12	-0.03	0.46	0.00	0.00	0.00	0.06	0.00	-0.30	-0.62					
Flow rates through the boundaries	Variance Log $K$	-0.49	-0.46	-0.41	-0.06	-0.17	-0.02	-0.05	-0.05	-0.01	0.39	0.00	0.01	0.00	0.06	0.00	0.29	-0.24					
	Average $K$	-0.05	0.13	0.11	0.01	0.06	0.00	0.01	0.03	0.00	-0.15	0.00	0.00	0.00	-0.03	0.00	-0.01	0.19					
	Variance $K$	0.09	0.46	0.43	0.03	0.16	0.01	0.04	0.07	0.01	-0.44	0.00	0.00	0.00	-0.08	0.00	0.06	-0.59					
Statistics of $K^{(est)}$	Average Log $K$	0.01	0.45	0.45	0.04	0.14	0.01	0.04	0.08	0.01	-0.44	0.00	0.00	0.00	-0.08	0.00	0.06	-0.58					
	Variance $K$	0.33	0.45	0.40	0.04	0.20	0.01	0.05	0.02	0.00	-0.39	0.00	0.00	0.00	-0.07	0.00	0.06	-0.56					
	Variance Log $K$	-0.40	-0.44	-0.38	-0.04	-0.21	-0.01	-0.05	-0.01	0.00	0.36	0.00	0.00	0.00	0.07	0.00	-0.06	0.54					

(c)



(d)

Fig. 14 - Results for the sensitivity indicator  $S_i^\sigma$  (a). Results for the sensitivity indicator  $ps_s$ ; (b). Results for the sensitivity indicator  $S_i$  (c). Values of the  $S_i$  indicator for the most significant parameters (d).

Fig. 14 - Risultati dell'indicatore di sensibilità  $S_i^\sigma$  (a). Risultati dell'indicatore di sensibilità  $ps_s$ ; (b). Risultati dell'indicatore di sensibilità  $S_i$  (c). Valori dell'indicatore  $S_i$  relativi ai parametri maggiormente significativi (d).

incoming flows through the boundary between Salento and the Murge hills and through the Ionian coast, but it does not influence the statistics related to the  $K^{(est)}$  field, despite the problems related to the non-uniqueness of solution of the inverse problem. Furthermore, possible variations on  $C$  could influence the flows through the boundary of the domain, while  $\delta$  mainly influences the volume of the aquifer saturated with fresh water.

## Conclusions

In this paper, a numerical model was applied to simulate water flow in the deep carbonate aquifer of Salento, consisting of fractured and karst rocks: this is the main water resource of the peninsula, and is exploited mainly for irrigation purposes and, to a less limited extent, for drinking purposes.

For the realization of the numerical flow model, a reconstruction of the hydrostratigraphic architecture of the study area was fundamental, in order to properly take into account the relationship between groundwater and seawater.

The revision of a previous version of the conceptual model yields an improvement of the hydrostratigraphic set up: in fact, it is now considered that the top of the main regional aquifer is given by the top of the Gravina calcarenites unit, where it is in direct contact with the Cretaceous Altamura sandstone, without the interposition of any low permeability geological formations. Then, the identification of the reference head field was also improved, by a even more careful analysis of the original data set at some critical areas.

Both the conceptual and the numerical models show that the aquifer is mainly fed from groundwater flow from the Murge hills and rain infiltration and discharges into the sea through the Ionian and the Adriatic coasts. Furthermore, the numerical model correctly identifies the areas where the aquifer is saturated with salt water and provides information about the global balance of the aquifer itself.

Since some of the model parameters are affected by high uncertainty, a sensitivity analysis was applied to assess how the variations around the reference values of the input parameters may influence the most significant model outcomes. In particular, from this analysis it was possible to deduce that the flows through the domain boundaries and the volume of the aquifer saturated with fresh water are the output parameters mostly influenced by possible variations of  $K^{(CM)}$ ,  $C$  and  $\delta$ .

The numerical model might have a considerable value for the management of groundwater resources of the region: in fact, it can be used to quantify possible effects of variations of the input parameters, related either to climate change or to human activities. Two examples of the application of the model are given here. In particular, the model is used to quantify the consequences that a decrease of the mean annual rainfall (natural change) or an increase of extractions for irrigation purposes (man induced change) are expected to have in terms of depletion and deterioration of groundwater quality. In both cases, the model predicts a lowering of hydraulic head in the central part of the peninsula and an increase of the extension of the area where the aquifer is saturated with salt water

(Fig.15). Therefore these simple tests show that the developed model can be a useful tool to guide a careful management of water resources of the region, because it easily provides a fast assessment of how and to what extent the modification of the exploitation of the aquifer might impact on the main water resource of the area, in terms of both quantity and quality.

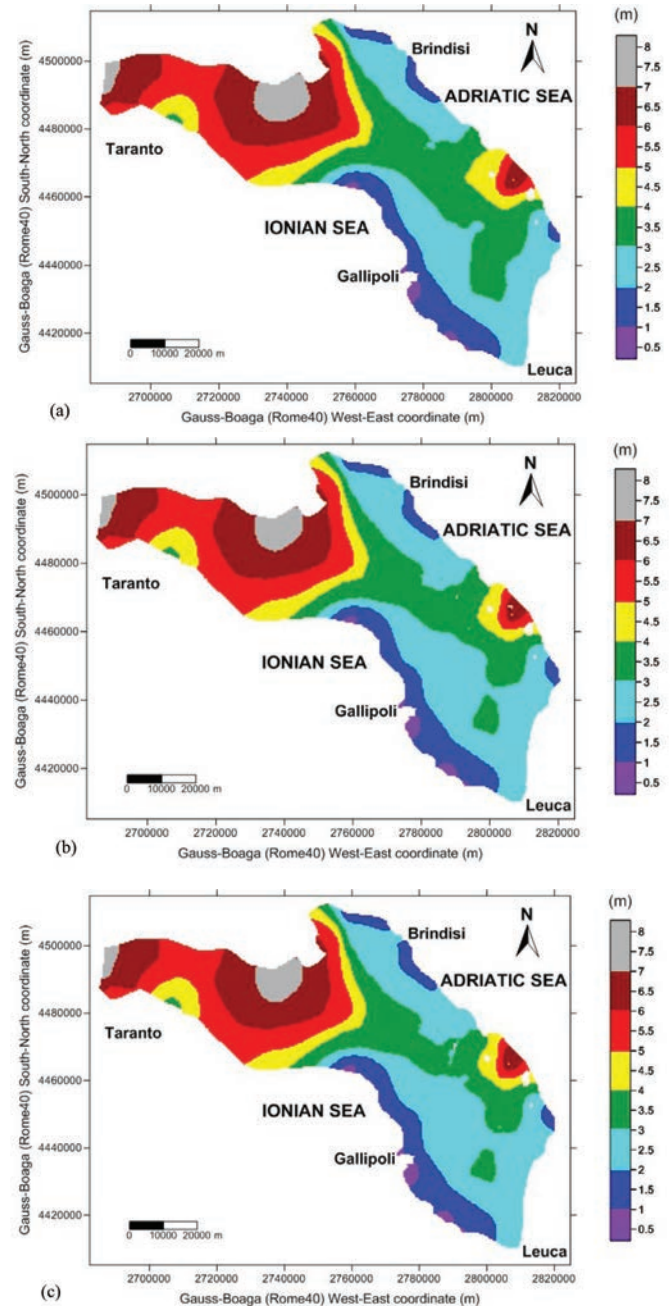


Fig. 15 - Comparison between (a) the piezometric head estimated for the heterogeneous medium obtained for the reference test, (b) that obtained by varying the input parameter "Rain" of a quantity  $\Delta x = -0.1x_{ref}$  and (c) that obtained by varying the input parameter "Irrigation vineyards" of a quantity  $\Delta x = +0.2x_{ref}$ .

Fig. 15 - Confronto tra (a) l'altezza piezometrica stimata con il mezzo eterogeneo ottenuta per la prova di riferimento, (b) quella ottenuta variando il parametro di ingresso "Pioggia" di una quantità  $\Delta x = -0.1x_{ref}$  e (c) quella ottenuta variando il parametro di ingresso "Irrigazione vigneti" di una quantità  $\Delta x = +0.2x_{ref}$ .

**Acknowledgements:** This work has been partially funded by the Flagship Project RITMARE - The Italian Research for the Sea - coordinated by the Italian National Research Council and funded by the Italian Ministry of Education, University and Research within the National Research Program 2011-2013.

## References

- Andreo B., Duràn J.J. (2008). Theme issue on groundwater in Mediterranean countries. *Environ. Geol.*, 54: 443-444, doi: 10.1007/s00254-007-0848-x.
- Bakalowicz M., El Hakim M., El-Hajj A. (2008). Karst groundwater resources in the countries of eastern Mediterranean: the example of Lebanon. *Environ. Geol.*, 54: 597-604, doi: 10.1007/s00254-007-0854-z.
- Baratelli F., Giudici M., Vassena C. (2012). A sensitivity analysis for an evolution model of the Antarctic ice sheet. *Reliability Engineering and System Safety*, 107: 64-70, doi:10.1016/j.res.2011.07.003.
- Bear J. (1979). *Hydraulics of groundwater*. McGraw-Hill.
- Cattaneo L., Giudici M., Vassena C. (2012). Modeling groundwater flow in heterogeneous media with YAGMod, Abstract FLOW-PATH 2012 Percorsi di Idrogeologia, I edizione, Bologna.
- Church M.R., Bishop G.D., Cassell D.L. (1995). Maps of regional evapotranspiration and runoff precipitation ratios in the northeast United States. *Journal of Hydrogeology*, 168: 283-298.
- Cotecchia V., Grassi D., Polemio M. (2005). Carbonate aquifers in Apulia and seawater intrusion. *Giornale di Geologia Applicata*, 1: 219-231, doi:10.1474/GGA.2005-01.0-22.0022.
- Custodio E. (2010). Coastal aquifers in Europe: an overview. *Hydrogeology Journal*, 18: 269-280, doi: 10.1007/s10040-009-0496-1.
- Daskalaki P., Voudouris K. (2008). Groundwater quality of porous aquifers in Greece: a synoptic review. *Environ. Geol.*, 54: 505-513, doi: 10.1007/s00254-007-0843-2.
- Davraz A., Karaguzel R., Soyaşlan I., Sener E., Seyman F., Sener S. (2009). Hydrogeology of karst aquifer systems in SW Turkey and an assessment of water quality and contamination problems. *Environ. Geol.*, 58: 973-988, doi: 10.1007/s00254-008-1577-5.
- De Filippis G. (2012). Modellazione numerica del flusso idrico nell'acquifero carbonatico del Salento: analisi di sensibilità "Numerical modeling of groundwater flow in the karst aquifer of Salento: sensitivity analysis". Tesi di Laurea Magistrale.
- Delle Rose M., De Marco M., Federico A., Fidelibus C., Internò G., Orgiato W., Piscazzi A. (2003). Studio preliminare sul rischio di desertificazione nel territorio carsico di Lecce "Preliminary study on the risk of desertification in the karst area of Lecce". Atti II convegno Il carsismo nell'area mediterranea.
- El-Bihery M.A. (2009). Groundwater flow modeling of Quaternary aquifer Ras Sudr, Egypt. *Environ. Geol.*, 58: 1095-1105, doi: 10.1007/s00254-008-1589-1.
- Giudici M., Vassena C. (2008). Spectral analysis of the balance equation of ground water hydrology. *Transp Porous Med*, 72: 171-178, doi:1007/s11242-007-9142-3.
- Giudici M., Margiotta S., Mazzone F., Negri S., Vassena C. (2012a). Modelling hydrostratigraphy and groundwater flow of a fractured and karst aquifer in a Mediterranean basin (Salento peninsula, southeastern Italy). *Environmental Earth Sciences*, doi:10.1007/s12665-012-1631-1.
- Giudici M., Baratelli F., Castellani G., Vassena C. (2012b). Modeling the Antarctic ice sheet and ice shelves: assessing the effects of uncertainty on the model parameters by sensitivity analysis. In: *Ice Sheets: Dynamics, Formation and Environmental Concerns* (Müller J. and Koch L., Eds.), 121-142. Nova Science Publishers, Inc., Hauppauge, N.Y.
- Hill M., Tiedeman C. (2006). *Effective groundwater model calibration: with analysis of data, sensitivities, predictions and uncertainty*. John Wiley & Sons.
- Lin J., Blake Snodsmith J., Zheng C., Wu J. (2009). A modeling study of seawater intrusion in Alabama Gulf Coast, USA. *Environ. Geol.*, 57: 119-130, doi: 10.1007/s00254-008-1288-y.
- Margiotta S., Negri S. (2004). Alla ricerca dell'acqua perduta "In search of lost water". Congedo Editore.
- Margiotta S., Negri S. (2005). Geophysical and stratigraphical research into deep groundwater and intruding seawater in the mediterranean area (the Salento Peninsula, Italy). *Natural Hazards and Earth System Sciences*, 5: 127-136.
- Polemio M., Limoni P.P., Mitolo D., Virga R. (2006). Il degrado qualitativo delle acque sotterranee pugliesi "The deterioration in quality of apulian groundwater". *Giornale di Geologia Applicata*, 3: 25-31, doi:10.1474/GGA.2006-03.0-03.0096.
- Polemio M., Dragone V., Limoni P.P., Romanazzi A. (2012). Metodologie speditive per la valutazione del rischio di degrado quantitativo e qualitativo delle acque sotterranee della Puglia "Speditive methodologies for assessing the risk of qualitative and quantitative deterioration of groundwater in Puglia". *Geologi e Territorio*, 1: 3-14.
- Ponzini G., Crosta G. (1988). The comparison model method: a new arithmetic approach to the discrete inverse problem of groundwater hydrology, 1, One-dimensional flow. *Transport in Porous Media*, 3: 415-436.
- Ponzini G., Lozej A. (1982). Identification of aquifer transmissivities: the comparison model method. *Water Resources Research*, 18: 597-622.
- Post V., Abarca E. (2010). Preface: saltwater and freshwater interactions in coastal aquifers. *Hydrogeology Journal*, 18: 1-4, doi: 10.1007/s10040-009-0561-9.
- Regione Puglia - Servizio Tutela della Acque (2009). *Relazione Generale-Piano di Tutela della Acque*.
- Saltelli A., Ratto M., Andres T., Campolongo F., Cariboni J., Gatelli D., et al. (2008). *Global sensitivity analysis - the primer*. Chichester, UK: John Wiley & Sons.
- Scarascia S., Ponzini G. (1972). An approximate solution for the inverse problem in hydraulics. *L'Energia Elettrica*, 49: 518-531.
- Simpson T.B., Holman I.P., Rushton K.R. (2010). Understanding and modelling spatial drain-aquifer interactions in a low-lying coastal aquifer - the Thurne catchment, Norfolk, UK. *Hydrological Processes*, 25: 580-592, doi: 10.1002/hyp.7845.
- Vandenbohede A., Van Houtte E., Lebbe L. (2009). Sustainable groundwater extraction in coastal areas: a Belgian example. *Environ. Geol.*, 57: 735-747, doi: 10.1007/s00254-008-1351-8.
- Younger P.L. (1996). Submarine groundwater discharge. *Nature*, 382: 121-122.
- Yuan D., Lin B. (2009). Modelling coastal ground- and surface-water interactions using an integrated approach. *Hydrological Processes*, 23: 2804-2817, doi: 10.1002/hyp.7377.